JOURNAL OF VIROLOGY, Apr. 2005, p. 4651–4663 Vol. 79, No. 8
0022-538X/05/$08.00+0 doi:10.1128/JVI.79.8.4651–4663.2005

Activation of CD21 and CD23 Gene Expression by Kaposi's Sarcoma-Associated Herpesvirus RTA

Heesoon Chang,[1] Yousang Gwack,[1] Dior Kingston,[1] John Souvlis,[1] Xiaozhen Liang,[1] Robert E. Means,[1] Ethel Cesarman,[2] Lindsey Hutt-Fletcher,[3] and Jae U. Jung[1]*

Department of Microbiology and Molecular Genetics and Tumor Virology Division, New England Primate Research Center, Harvard Medical School, Southborough, Massachusetts[1]; Department of Pathology, Weil Medical College, Cornell University, New York, New York[2]; and Department of Microbiology and Immunology, Louisiana State University Health Science Center, Shreveport, Louisiana[3]

Received 13 August 2004/Accepted 23 November 2004

Epstein-Barr virus (EBV) EBNA2 and Kaposi's sarcoma-associated herpesvirus (KSHV) replication and transcription activator (RTA) are recruited to their responsive elements through interaction with a Notch-mediated transcription factor, RBP-Jκ. In particular, RTA and EBNA2 interactions with RBP-Jκ are essential for the lytic replication of KSHV and expression of B-cell activation markers CD21 and CD23a, respectively. Here, we demonstrate that like EBV EBNA2, KSHV RTA strongly induces CD21 and CD23a expression through RBP-Jκ binding sites in the first intron of CD21 and in the CD23a core promoter, respectively. However, unlike EBV EBNA2, which alters immunoglobulin μ (Igμ) and c-*myc* gene expression, RTA did not affect Igμ and c-*myc* expression, indicating that KSHV RTA targets the Notch signal transduction pathway in a manner similar to but distinct from that of EBV EBNA2. Furthermore, RTA-induced expression of CD21 glycoprotein, which is an EBV receptor, efficiently facilitated EBV infection. In addition, RTA-induced CD23 glycoprotein underwent proteolysis and gave rise to soluble CD23 (sCD23) molecules in B lymphocytes and KSHV-infected primary effusion lymphocytes. sCD23 then stimulated primary human lymphocytes. These results demonstrate that cellular CD21 and CD23a are common targets for B lymphotropic gammaherpesviruses and that KSHV RTA regulates RBP-Jκ-mediated cellular gene expression, which ultimately provides a favorable milieu for viral reproduction in the infected host.

Kaposi's sarcoma-associated herpesvirus (KSHV), also called human herpesvirus 8, is thought to be an etiologic agent of Kaposi's sarcoma (KS) (4). KSHV is also associated with two diseases of B-cell origin: primary effusion lymphoma (PEL) and an immunoblast variant of Castleman disease (2, 3). An important step in the herpesvirus life cycle is the switch from latency to lytic replication. The KSHV replication and transcription activator (RTA) plays a central role in this switch. Ectopic expression of KSHV RTA is sufficient to disrupt viral latency and activate lytic replication to completion (8, 23, 35, 38). RTA activates the expression of numerous viral genes in the lytic cycle of KSHV, including its own promoter, polyadenylated nuclear RNA, K12, ORF57, vOX-2, viral G-protein-coupled receptor, and vIRF1. While the details of RTA-mediated transcriptional activation remain unclear, several pieces of evidence suggest that RTA activates its target promoter through direct binding to the specific sequence (20) and/or interaction with various cellular transcriptional factors. In fact, numerous cellular proteins, such as Stat3, KRBP, RBP-Jκ/CBF1, and CBP, interact with RTA, and these interactions act synergistically with RTA transcriptional activity (10, 11, 18, 19, 32, 44). Furthermore, our recent study (9) demonstrated that RTA recruits cellular SWI/SNF and TRAP/mediator complexes through its carboxy-terminal short acidic sequence. Recruitment of these complexes onto viral lytic promoters is essential for their effects on target promoters and KSHV reactivation (9).

Epstein-Barr virus (EBV) EBNA2 and KSHV RTA have been shown to be recruited to their responsive elements through interaction with the transcription factor RBP-Jκ (13, 18, 21). RBP-Jκ binding sites are present in a number of EBNA2- and RTA-regulated viral promoters. RBP-Jκ, which was originally purified and characterized by Kawaichi et al. (17) and Hamaguchi et al. (12), has been highly conserved in the evolution from nematodes to humans. Biochemical and genetic studies have demonstrated that RBP-Jκ acts downstream of the receptor Notch. Activation of the Notch receptor by binding of its ligands (Delta, Jagged, or Serrate) leads to proteolytic cleavage of the receptor at the inner side of the membrane (30). The Notch intracellular domain (NIC) is then translocated to the nucleus, where it activates genes by interacting with RBP-Jκ. EBNA2 and RTA may thus be regarded as functional homologs or mimics of the activated Notch protein. Indeed, NIC has been shown to be capable of functionally substituting for EBNA2 in the context of EBV for primary B-cell transformation (7). However, the cellular targets of cellular NIC do not completely overlap with those of EBNA2: EBNA2 and RTA both activate CD21 (CR2, EBV receptor) gene expression and repress immunoglobulin μ (Igμ) expression, whereas EBNA2, but not NIC, activates CD23a gene expression (37).

Despite detailed studies of RTA-mediated viral gene expression, the cellular targets of RTA have not been characterized.

* Corresponding author. Mailing address: Tumor Virology Division, New England Primate Research Center, Harvard Medical School, 1 Pine Hill Dr., Southborough, MA 01772. Phone: (508) 624-8083. Fax: (508) 786-1416. E-mail: jae_jung@hms.harvard.edu.

Here, we demonstrate that, similar to EBV EBNA2 and cellular NIC, KSHV RTA activates cellular CD21 and CD23a gene expression through their RBP-Jκ binding sites, resulting in drastic increases in the expression of CD21 and CD23a on the surfaces of RTA-expressing B cells and KSHV-infected PEL cells. RTA-mediated upregulation of CD21 surface expression consequently results in the enhancement of EBV infection, while upregulation of CD23a results in the activation of primary lymphocytes. Thus, RTA interacts with RBP-Jκ and strongly activates the expression of B-cell-specific surface molecules, which may offer a favorable environment for reproduction of KSHV and other viruses.

MATERIALS AND METHODS

Cell culture and transfection. 293T, BJAB, and BCBL-1 cells were grown in Dulbecco's modified Eagle's medium or RPMI 1640 medium supplemented with 10% fetal calf serum. EBV-infected B95 and AGS cells were induced with phorbol-12-tetradecanoate-13-acetate (TPA) (20 ng/ml) (Sigma, St. Louis, Mo.).

RNA extraction and reverse transcriptase PCR (RT-PCR). Total RNA (10 μg) was used for the synthesis of first strand cDNA according to the manufacturer's instructions. Aliquots of cDNA samples were then PCR amplified with a combination of forward and reverse gene-specific primers. The amplified PCR products were separated on 2% agarose gels, visualized by ethidium bromide staining, and photographed.

Microarray analysis. Total RNA was isolated from TRExBJAB-cDNA5 and TRExBJAB-RTA cells (stimulated and unstimulated) with the use of Trizol (Invitrogen). For each microarray, 20 μg of a RNA sample was processed according to the manufacturer's standard protocol (Affymetrix, Santa Clara, Calif.) and hybridized to an Affymetrix HGU95A chip. The data from two independent experiments were analyzed by using the Affymetrix Mass 5.0 software and Genespring software (Silicon Genetics, Redwood City, Calif.).

Quantitative real-time RT-PCR. Real-time PCR was performed by the following thermocycling protocol: (i) 1 cycle of 2 min at 50°C and 10 min at 95°C; and (ii) 40 cycles, with 1 cycle consisting of 15 s at 95°C and 1 min at 60°C. The primer pairs against CD21 (forward primer, GCCGACACGACTACCAACC; backward primer, AGCAAGTAACCAGATTCACAGC), CD23 (forward primer, GGAATTGAACGAGAGGAACGAAG; backward primer, AAAGCC GCTGGACACCTG), and β-actin (forward primer, AGGTGACAGCAGTCG GTTG; backward primer, TGGGGTGGCTTTTAGGATGG) were synthesized by Gene Link. Real-time PCR was completed with SYBR green PCR Master Mix and analyzed with MyQ software according to the manufacturer's instructions (Bio-Rad Instrument). For each primer pair, amplification efficiencies were determined by creating a standard curve; the log of the relative target quantity was plotted versus the cycle threshold value. The standard curves demonstrated various amplification efficiencies between primer pairs with slopes ranging from −3.6 to −3.3 representing amplification efficiencies between 90 and 100%, respectively. A dissociation curve was generated for each primer pair and demonstrated the amplification of a single product. The sizes of the amplified products were confirmed by agarose gel electrophoresis. Reactions were completed in duplicate, and no-template controls were included for each primer pair. The induction level of CD21 and CD23 expression in RTA-expressing cells was normalized to the β-actin transcript level and presented as fold induction compared with that in control cells.

Luciferase assay. Cells were transfected with pCD21-Luc and pCD21-Luc-Intron (kindly provided by J. H. Weis, University of Utah School of Medicine) (46) or CD23-AC-Luc and CD23-ACP-Luc (kindly provided by H. P. Tony, University of Wurzburg, Wurzburg, Germany) (41), β-galactosidase plasmid, and the indicated amount of empty vector, RTA expression vector, or NIC expression vector (kindly provided by P. Ling, Baylor College of Medicine) (7). At 48 h posttransfection, cells were washed twice with phosphate-buffered saline (PBS), lysed, and analyzed by luciferase assay (Promega, Madison, Wis.). Luciferase levels were normalized to β-galactosidase activity and presented as fold induction compared with the control.

EBV infection. EBVfaV-GFP and EBV-ΔTK-GFP were obtained after 5 days of stimulation of B95-EBVfaV-GFP cells (kindly provided by Rich Longnecker, Northwestern Medical School) (36) with TPA (20 ng/ml) or after stimulation of AGS-EBV-ΔTK-GFP cells (1) with butyric acid (3 mM). Viral suspensions were used to infect doxycycline (DOXY)-treated or untreated TRExBJAB-cDNA5 and TREXBJAB-RTA cells by incubating the virus suspension with 10^5 cells in a volume of 1 ml of complete RPMI 1640 medium containing TPA and butyric acid for 1 h at 37°C with vigorous agitation. At 48 h postinfection, BJAB cells were fixed and immunostained with anti-CD21, anti-CD23, anti-MHC-I (anti-major histocompatibility complex class I), or anti-MHC-II antibodies.

Flow cytometry. Cells (5×10^5) were washed with RPMI 1640 medium containing 10% fetal calf serum and incubated for 30 min with antibodies. Cells were then incubated for 20 min at 4°C with secondary anti-mouse antibodies (Pharmingen, San Diego, Calif.). After the cells were washed, each cell sample was fixed with 2% paraformaldehyde, and fluorescence-activated cell sorting analysis was performed with a FACScan (Becton Dickinson, Mountain View, Calif.).

ELISA of soluble CD23 (sCD23). Purified anti-CD23 antibody was diluted to 1 μg/ml in PBS (pH 7.5). Each well of a 96-well enzyme-linked immunosorbent assay (ELISA) plate (Dynex) was coated with 100 μl of the anti-CD23 solution in coating buffer (0.2 M sodium phosphate, pH 6.5) overnight at 4°C. The wells were blocked for 1 h with PBS supplemented with 1% bovine serum albumin. After the wells were blocked, they were washed with PBS containing 0.05% Tween 20 and incubated with the supernatants of DOXY-treated TRExBJAB-cDNA5 or TRExBJAB-RTA cells. The wells were washed with PBS containing 0.05% Tween 20 and incubated with alkaline phosphatase-conjugated goat anti-mouse Ig (diluted 1:4,000; Jackson Laboratory) for 1 h at room temperature. After the wells were washed, they were developed by the addition of *p*-nitrophenyl phosphate (Sigma) in diethanolamine substrate buffer (Pierce, Rockford, Ill.).

RESULTS

KSHV RTA activates CD21 and CD23a gene expression. To identify cellular genes activated by KSHV RTA, we compared the cellular transcriptional profiles of parental cells and cells expressing RTA. For this assay, we used KSHV- and EBV-negative BJAB cell lines (TRExBJAB-cDNA5 and TRExBJAB-RTA cells) in which the Myc epitope-tagged wild-type RTA gene was integrated into the chromosomal DNA under the control of a tetracycline-inducible promoter (27). Treating these cells with DOXY rapidly and strongly induced RTA expression. After DOXY treatment of TRExBJAB-cDNA5 cells and TRExBJAB-RTA cells for 0, 24, and 48 h, total RNAs were isolated and analyzed by using an Affymetrix microarray. Comparing the transcriptional profiles of TRExBJAB-cDNA5 cells and TRExBJAB-RTA cells to the profile of parental cells indicated that approximately 100 of 12,000 cellular genes were induced by at least threefold, and approximately 13 genes were repressed by at least twofold (Table 1). Of these cellular genes, the expression levels of CD21 and CD23a genes were consistently induced in TRExBJAB-RTA cells by 7- and 10-fold, respectively, after 24 h of DOXY treatment, and by 11- and 20-fold, respectively, after 48 h of DOXY treatment.

To confirm the induction of CD21 and CD23a gene expression by RTA, TRExBJAB-cDNA5 and TRExBJAB-RTA cells and KSHV-positive TRExBCBL1-cDNA5 and TRExBCBL1-RTA cells were treated with DOXY. After 0, 24, and 48 h of treatment, total RNAs were isolated and analyzed by RT-PCR to measure the expression of CD21 and CD23a genes. In addition, cellular actin, c-*myc*, and Igμ genes were included as controls. CD21 and CD23a mRNAs in TRExBJAB-RTA and TRExBCBL1-RTA cells were induced and remained at elevated levels after 48 h of treatment with DOXY (Fig. 1). In contrast, CD21 and CD23a mRNAs in TRExBJAB-cDNA5 and TREXBCBL1-cDNA5 cells stayed at low levels throughout the DOXY treatment (Fig. 1). Densitometry analysis indicated a twofold induction of CD21 and a three- to fivefold induction of CD23a mRNA in TRExBJAB-RTA and TREx BCBL1-RTA cells after 48 h of DOXY treatment.

Because of the weak sensitivity of RT-PCR analysis in quan-

TABLE 1. Summary of results of microarray analysis[a]

Gene	Accession no.	Fold change[b]
sparc/osteonectin, cwcv and kazal-like domains proteoglycan (testican)	AF231124	3.0
Plasma glutamate carboxypeptidase	NM_016134	3.0
Junctional adhesion molecule 2	NM_021219	3.0
Flavin-containing monooxygenase 3	NM_006894	3.0
Hypothetical protein DKFZp434P2235	AL136860	3.0
Zinc finger protein 278	AF254087	3.0
Fragile X mental retardation, autosomal homolog 1	AI990766	3.0
Transient receptor potential channel 1	NM_003304	3.0
Caspase 6, apoptosis-related cysteine protease	BC000305	3.0
Hypothetical protein FLJ20059	AW006750	3.0
CGI-127 protein	NM_016061	3.0
Lymphocyte antigen 95 (activating NK receptor; NK-p44)	NM_004828	3.0
MD-1, RP105-associated	NM_004271	3.0
CD53 antigen	NM_000560	3.0
Purinergic receptor P2X, ligand-gated ion channel 1	U45448	3.0
Pellino homolog 2 (*Drosophila*)	NM_021255	3.0
Hypothetical protein FLJ22344	NM_024717	3.1
Cystathionase (cystathionine γ-lyase)	NM_001902	3.1
KIAA0740 gene product	AB018283	3.1
Vascular endothelial growth factor	AF022375	3.1
RAB-8b protein	NM_016530	3.1
Glutathione *S*-transferase M2 (muscle)	NM_000848	3.1
Ryanodine receptor 3	NM_001036	3.1
B-cell translocation gene 1, antiproliferative	AL535380	3.1
Chemokine (C-C motif) receptor 7	NM_001838	3.1
Acid phosphatase, prostate	NM_001099	3.2
Programmed cell death 4 (neoplastic transformation inhibitor)	NM_014456	3.2
FK506 binding protein 5	NM_004117	3.2
ADP-ribosylation factor 1	AA580004	3.2
Programmed cell death 4 (neoplastic transformation inhibitor)	NM_014456	3.2
Microtubule-associated protein tau	J03778	3.2
Polymerase (RNA) II (DNA-directed) polypeptide E (25 kDa)	AI554759	3.3
Solute carrier family 21 (organic anion transporter), member 11	BC00585	3.3
H3 histone family, member K	NM_003536	3.3
RagD protein	AF272036	3.3
KIAA0620 protein	AL575403	3.3
Sialic acid binding Ig-like lectin 8	NM_014442	3.4
Poly(A) polymerase gamma	NM_022894	3.4
LPS-induced TNF-α[c]	AB034747	3.4
Hairy/enhancer-of-split related with YRPW motif 1	NM_012258	3.4
Growth arrest and DNA-damage-inducible, alpha	NM_001924	3.5
Glutathione *S*-transferase M1	X08020	3.5
Villin 2 (ezrin)	AF199015	3.6
Basigin (OK blood group)	AL550657	3.6
Crystallin, mu	NM_001888	3.6
Putative UDP-GalNAc:polypeptide *N*-acetylgalactosaminyltransferase T9	BE906572	3.7
Thioredoxin-interacting protein	AA812232	3.7
UDP-GlcNAc:β-Gal β-1,3-*N*-acetylglucosaminyltransferase 1	NM_006577	3.8
Basement membrane-induced gene	NM_004848	3.8
Hydroxyacyl-coenzyme A dehydrogenase/3-ketoacyl-coenzyme A Thiolase/enoyl-coenzyme A hydratase, alpha subunit	BG472176	3.8
SH3-domain, GRB2-like, endophilin B2	NM_020145	3.8
Secreted protein, acidic, cysteine-rich (osteonectin)	NM_003118	3.9
Zinc finger homeobox 1B	NM_014795	3.9
Tropomodulin	BC002660	3.9
Lysophosphatidic acid phosphatase	NM_016361	3.9
Syntrophin, gamma 2	NM_018968	4
Phorbolin-like protein MDS019	NM_021822	4.1
Guanine nucleotide binding protein (G protein), gamma 7	NM_005145	4.2
Scaffold attachment factor B	AI769566	4.2
Tropomodulin	NM_003275	4.2
Interleukin 1 receptor, type II	U64094	4.2
BCL2-like 1	U72398	4.2
Myeloid or lymphoid or mixed-lineage leukemia; translocated to 2	NM_005935	4.3
ATP-binding cassette, subfamily B (MDR/TAP), member 4	NM_000443	4.3
RNase 6 precursor	NM_003730	4.4
Insulin-like growth factor binding protein 6	NM_002178	4.5
Hemopoietic cell kinase	NM_002110	4.6
Stress-induced-phosphoprotein 1 (Hsp70/Hsp90-organizing protein)	AL553320	4.6
CD22 antigen	X52785	4.6
Hypothetical protein FLJ20607	NM_017899	4.7
Integrin, beta 7	NM_000889	4.8

Continued on following page

TABLE 1—*Continued*

Gene	Accession no.	Fold change[b]
OLF-1/EBF-associated zinc finger gene	AW149417	4.9
H2A histone family, member O	AI313324	5.2
Kinesin-like 4	AC002301	5.5
Anaphase-promoting complex subunit 5	BF967271	5.5
Translocase of inner mitochondrial membrane 10 homolog (yeast)	AI082078	5.9
Myosin binding protein C, slow type	BF593509	6.1
Glutathione *S*-transferase M4	M99422	6.1
Palladin	AU157932	6.2
Lymphocyte cytosolic protein 2	NM_005565	6.4
Small inducible cytokine A3	NM_002983	6.5
Transcription factor 3	AA768906	6.6
Myosin, light polypeptide 3, alkali; ventricular, skeletal, slow	NM_000258	6.9
Neurturin	AL161995	7
Nuclear factor I/B	BC001283	7.1
Inhibitor of DNA binding 1, dominant-negative helix-loop-helix protein	D13889	7.6
Neutrophil cytosolic factor 2	BC001606	7.6
Chitinase 3-like 2	U58515	7.8
Inactive progesterone receptor, 23 kDa	BE903880	8.1
Solute carrier family 1, member 1	AW235061	8.5
Mitogen-activated protein kinase kinase 2	AI762811	8.7
Natural killer cell receptor 2B4	NM_016382	9.2
Eukaryotic translation initiation factor 5A	NM_001970	9.3
C-type lectin, superfamily member 6	AF200738	9.5
CD21 (complement component 3d or EBV) receptor 2	**NM_001877**	**11**
Enolase 1, (alpha)	U88968	14.3
CD23a (Fc fragment of IgE, low-affinity II, receptor for CD23a receptor for CD23a)	**NM_002002**	**20**
Sjogren syndrome antigen B (autoantigen La)	BG532929	−3.7
Origin recognition complex, subunit 5-like (yeast)	AF081459	−3.1
UDP-Gal:βGlcNAc β-1,3-3-galactosyltransferase, polypeptide 3	AB050855	−3.1
Fyn-related kinase	NM_002031	−3.0
Aldehyde dehydrogenase 1 family, member A1	NM_000689	−2.9
C-terminal binding protein 1	BF984434	−2.7
Novel putative protein similar to YIL091C yeast hypothetical 84-kDa protein	AI770084	−2.7
Tumor necrosis factor receptor superfamily, member 17	NM_001192	−2.6
Caldesmon 1	NM_004342	−2.5
Bromodomain adjacent to zinc finger domain, 1A	AA102574	−2.5
Pre-B-lymphocyte gene 3	NM_013378	−2.4
v-myb myeloblastosis viral oncogene homolog (avian)-like 1	AW592266	−2.2
KIAA0974 protein	AW241779	−2.1

[a] The CD21 and CD23a entries are shown in bold type, as they gave the highest fold changes compared to the values from parental cells.
[b] Fold change compared to the value for parental cells.
[c] LPS, lipopolysaccharide; TNF-α, tumor necrosis factor alpha.

titation, real-time RT-PCR was performed on RNAs from DOXY-treated or untreated TRExBJAB-cDNA5 and TREx BJAB-RTA cells with the primers for cellular CD21, CD23a, and β-actin transcripts. It showed that CD21 and CD23a mRNA levels remained low in control TRExBJAB-cDNA5 cells for both DOXY-treated cells and untreated cells (Fig. 1B). In striking contrast, the levels of CD21 and CD23a mRNA were greatly increased in TRExBJAB-RTA cells upon DOXY treatment: the mRNA levels of CD21 and CD23a genes were induced by 160- and 23-fold, respectively, after 24 h of DOXY treatment, and by 40- and 20-fold, respectively, after 48 h of DOXY treatment (Fig. 1B). Interestingly, the level of CD21 mRNA peaked at 24 h of DOXY treatment and declined to the basal level at 48 h of DOXY treatment, whereas CD23a mRNA remained at elevated levels after 48 h of DOXY treatment, showing the different kinetics between RTA-mediated CD21 and CD23a mRNA induction. It should be noted that CD21 and CD23a expression was detected at a high level in untreated TRExBJAB-RTA cells because of the leakiness of DOXY-induced RTA expression (Fig. 1B). Finally, cellular c-*myc* and Igμ expression that is altered by EBV EBNA2 and cellular NIC (37) was examined by RT-PCR and immunoblot analyses. These analyses showed that unlike EBV EBNA2 and cellular NIC, KSHV RTA did not induce a detectable level of alteration in c-*myc* or Igμ gene expression (Fig. 1A and data not shown). Cellular actin and tubulin controls were also unchanged by DOXY treatment (Fig. 1A).

To further demonstrate the RTA-mediated induction of CD21 and CD23a, their level of surface expression was measured by flow cytometry. KSHV-negative TRExBJAB-cDNA5 and TRExBJAB-RTA cells and KSHV-positive TRExBCBL1-cDNA5 and TRExBCBL1-RTA cells were treated with DOXY for 0, 24, and 48 h, fixed with paraformaldehyde, and allowed to react with anti-CD21 and anti-CD23a antibodies. Anti-MHC-I, anti-MHC-II, anti-Igμ, and anti-ICAM1 antibodies were included as controls. The levels of CD21 and CD23a expressed on the cell surfaces of TRExBJAB-RTA cells increased by 10- and 1,000-fold after 48 h of DOXY treatment,

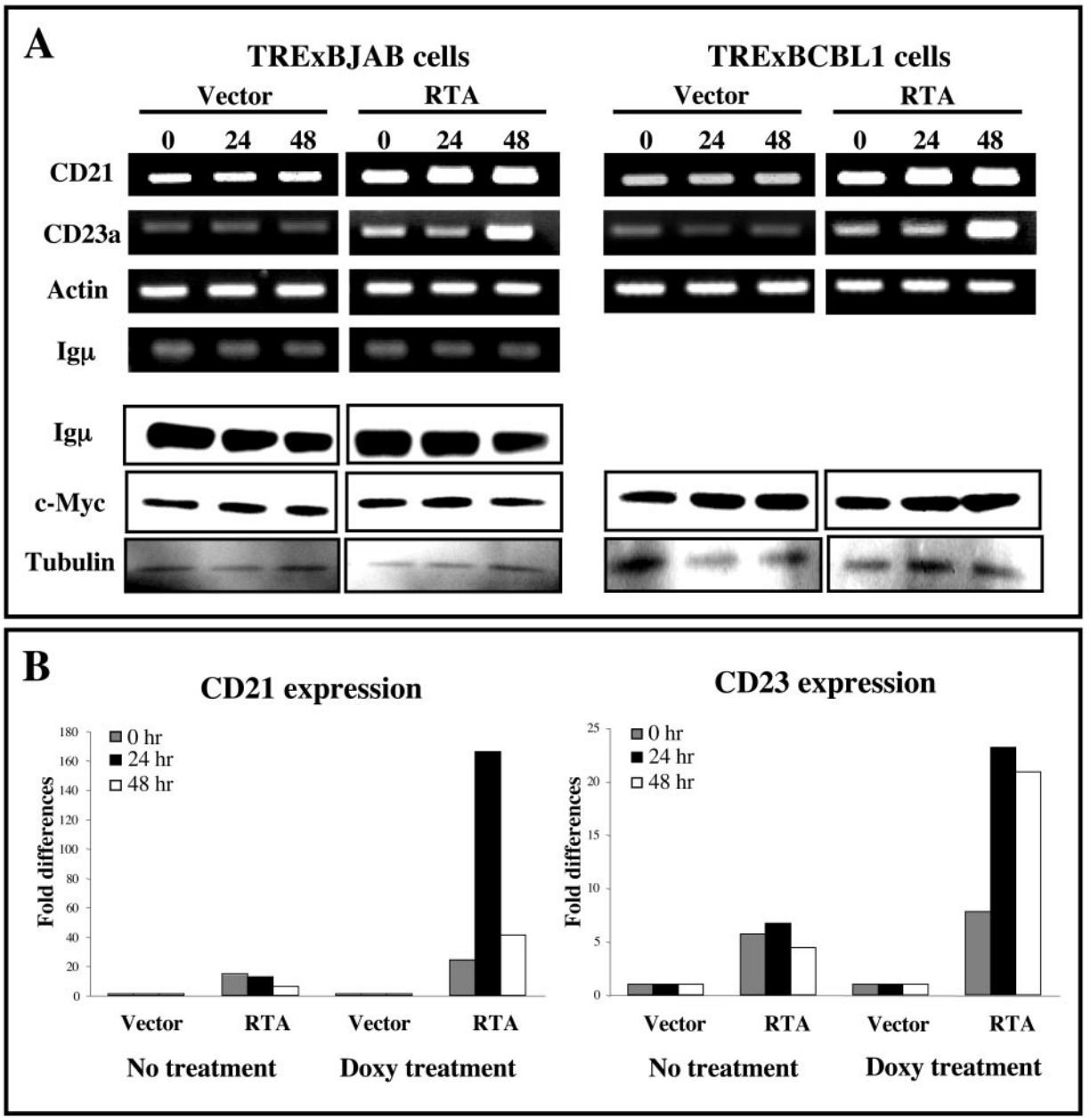

FIG. 1. Induction of CD21 and CD23a gene expression. (A) RT-PCR and immunoblot analyses of cellular gene expression induced by RTA. (Top) TRExBJAB-cDNA5, TRExBJAB-RTA, TRExBCBL1-cDNA5, and TRExBCBL1-RTA cells were stimulated with DOXY (1 μg/ml) for 0, 24, or 48 h or left alone. Total RNA was purified from each sample and used for RT-PCR analysis of the indicated genes. PCR mixtures were analyzed by agarose gel electrophoresis. TRExBCBL1-cDNA5 and TRExBCBL1-RTA cells showed no Igμ expression (data not shown). Total RNA purification and RT-PCR were repeated at least three times independently with similar results. (Bottom) Cells were stimulated with DOXY (1 μg/ml) or left alone as described above and analyzed by immunoblotting with anti-c-*myc* and antitubulin antibodies. (B) Quantitative real-time RT-PCR analysis. TRExBJAB-cDNA5 and TRExBJAB-RTA cells were stimulated with DOXY (1 μg/ml) for 0, 24, or 48 h or left alone. Quantitative real-time RT-PCR of CD21, CD23a, and β-actin mRNA was performed with RNA isolated as described in Materials and Methods. The results are presented as the fold induction of the value obtained for the RNA sample from TRExBJAB-RTA cells to the value obtained from RNA from TREx-BJAB-cDNA5 cells. The ratios were also normalized to the β-actin transcript level.

respectively (Fig. 2). In contrast, their surface expression was not altered on TRExBJAB-cDNA5 control cells (Fig. 2A). In addition, the surface expression of MHC-I, MHC-II, Igμ, and ICAM1 were not altered on either cell type with or without DOXY treatment, indicating that RTA specifically induced the surface expression of CD21 and CD23a (Fig. 2A and data not shown). When KSHV-positive TRExBCBL1-cDNA5 and TRExBCBL1-RTA cells were tested in the same assay, the surface expression of CD21 and CD23a increased only on TRExBCBL1-RTA cells, but not on TRExBCBL1-cDNA5 cells (Fig. 2B). However, we noticed that the levels of CD21 and CD23a expressed on the cell surface induced by RTA were

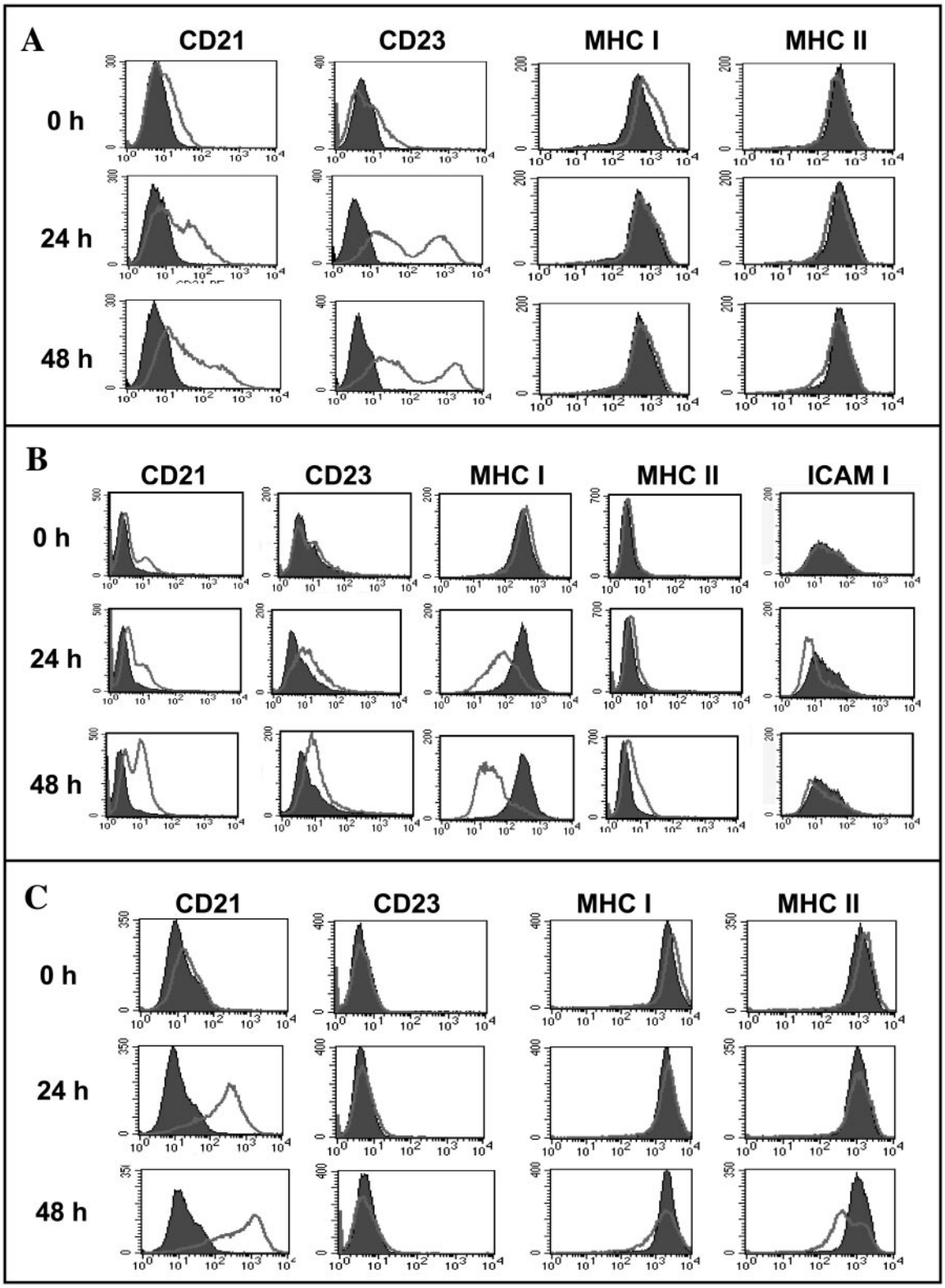

FIG. 2. Upregulation of CD21 and CD23 surface expression induced by RTA. TRExBJAB-cDNA5 and TRExBJAB-RTA cells (A), TREx BCBL1-cDNA5 and TRExBCBL1-RTA cells (B), and TRExBJAB-cDNA5 and TRExBJAB-NIC cells (C), were treated with 1 μg of DOXY per ml for 0, 12, and 48 h, fixed, and then reacted with the indicated antibodies for flow cytometry. The values for control TRExBJAB-cDNA5 and TRExBCBL1-cDNA5 cells (dark gray histograms) and TRExBJAB-RTA, TRExBCBL1-RTA, and TRExBJAB-NIC cells (light gray lines) are indicated.

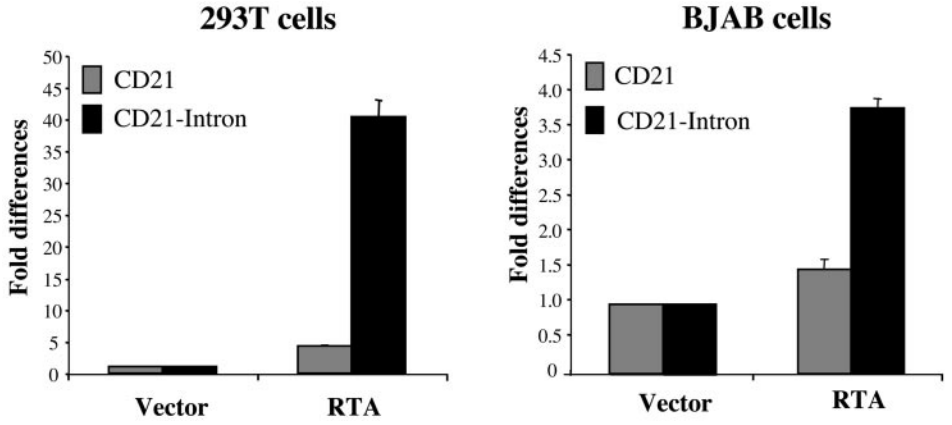

FIG. 3. Activation of CD21 promoter activity by RTA. 293T and BJAB cells were transfected with pCD21-Luc (CD21) or pCD21-Luc-Intron (CD21-Intron) reporter together with empty vector or RTA expression vector. Cotransfection with pGK-β-Gal provided a control reporter for transfection efficiency. At 48 h posttransfection, cell lysates were used for luciferase and β-galactosidase assays. Luciferase activity is presented as the average ± standard deviation (error bar) of three independent experiments.

lower on TRExBCBL1-RTA cells than on TRExBJAB-RTA cells (Fig. 2). Furthermore, unlike TRExBJAB-RTA cells on which MHC-I and ICAM1 were not affected by RTA expression, TRExBCBL1-RTA cells displayed a considerable reduction of MHC-I and ICAM1 surface expression upon DOXY treatment (Fig. 2B). The reduction of MHC-I and ICAM1 surface expression was likely mediated by KSHV K3 and K5 proteins, and the levels of expression of K3 and K5 proteins were induced by RTA-initiated lytic replication (5, 16).

To compare RTA with cellular NIC in the regulation of CD21 and CD23 surface expression, cellular NIC was also placed under the control of the DOXY-inducible promoter in TRExBJAB cells. Immunoblotting analysis showed that NIC expression was strongly induced upon DOXY treatment of the TRExBJAB-NIC cells (data not shown). These cells were treated with DOXY for 0, 24, and 48 h, fixed with paraformaldehyde, and allowed to react with ant-CD21, anti-CD23a, anti-MHC-I, and anti-MHC-II antibodies. Flow cytometry showed that NIC expression strongly induced CD21 surface expression in a tetracycline-inducible manner, whereas it did not induce CD23a surface expression under the same conditions (Fig. 2C). Furthermore, TRExBJAB-NIC cells showed no alteration of MHC-I surface expression and a slight reduction of MHC-II surface expression after 48 h of DOXY treatment (Fig. 2C). In summary, KSHV RTA and EBV EBNA2 induce cellular CD21 and CD23a gene expression, whereas cellular NIC induces only CD21 gene expression. Both EBV EBNA2 and cellular NIC alter c-*myc* and Igμ expression (37), whereas RTA does not affect Igμ and c-*myc* gene expression. These results collectively indicate that KSHV RTA targets the Notch-mediated signal transduction pathway in a manner similar to but distinct from those of EBV EBNA2 and cellular NIC.

RTA activates CD21 promoter activity through its intronic silencer. While EBV EBNA2 activates cellular CD21 gene expression (47), the detailed mechanism has not been elucidated. Recent studies have indicated that cell- and stage-specific expression of CD21 is regulated by an intronic transcriptional silencer sequence (24) and that this intronic transcriptional silencer sequence contains a binding site for the transcriptional repressor RBP-Jκ (14). To identify the RTA-mediated elements responsible for the activation of human CD21 expression, reporter constructs pCD21-Luc and pCD21-Luc-Intron were used to measure the transcription activity of CD21. pCD21-Luc contained the 5′-proximal promoter region of the CD21 gene (1,272 bp 5′ of the initiating ATG codon), and pCD21-Luc-Intron contained the additional 1.6 kb of intron 1 (14).

To determine the effect of RTA activity on the CD21 promoter, 293T and BJAB cells were transfected with pCD21-Luc or pCD21-Luc-Intron reporter together with vector alone or RTA expression vector. The pGK-β-Gal reporter was also included as a control for transfection efficiency. At 48 h posttransfection, cell lysates were used for luciferase and β-galactosidase assays. RTA was not able to activate the promoter activity of pCD21-Luc in either 293T or BJAB cells, whereas it efficiently activated the promoter activity of pCD21-Luc-Intron under the same conditions (Fig. 3). Note that a low level of CD21-Luc-Intron promoter activation was detected in BJAB cells. This was probably because of the presence of a B-cell-type-specific repressor element, the E-box motif, in the CD21 proximal promoter region; cellular E2A repressor binds to this motif and inhibits CD21 gene expression in a B-cell-specific manner (40). Nevertheless, these results indicate that RTA is recruited to the RBP-Jκ binding site in the first intron of CD21 to activate its transcription.

RTA-mediated activation of CD21 surface expression enhances EBV infection. Most cell lines derived from PEL are coinfected with EBV and KSHV, suggesting a potential cooperation between EBV and KSHV in their infection and/or pathogenesis (26). The initial event required for EBV entry into B cells is the interaction of the major viral envelope gp350/220 glycoprotein with its primary receptor, CD21, while this interaction is not necessary for epithelial infection (6, 29). Since RTA efficiently activated CD21 gene expression, we examined whether the activation of CD21 gene expression by RTA facilitates EBV infection. To test this hypothesis, we used three pairs of EBV-producing cells: B95 B lymphoma cells in which the LMP2A gene had been replaced with the green

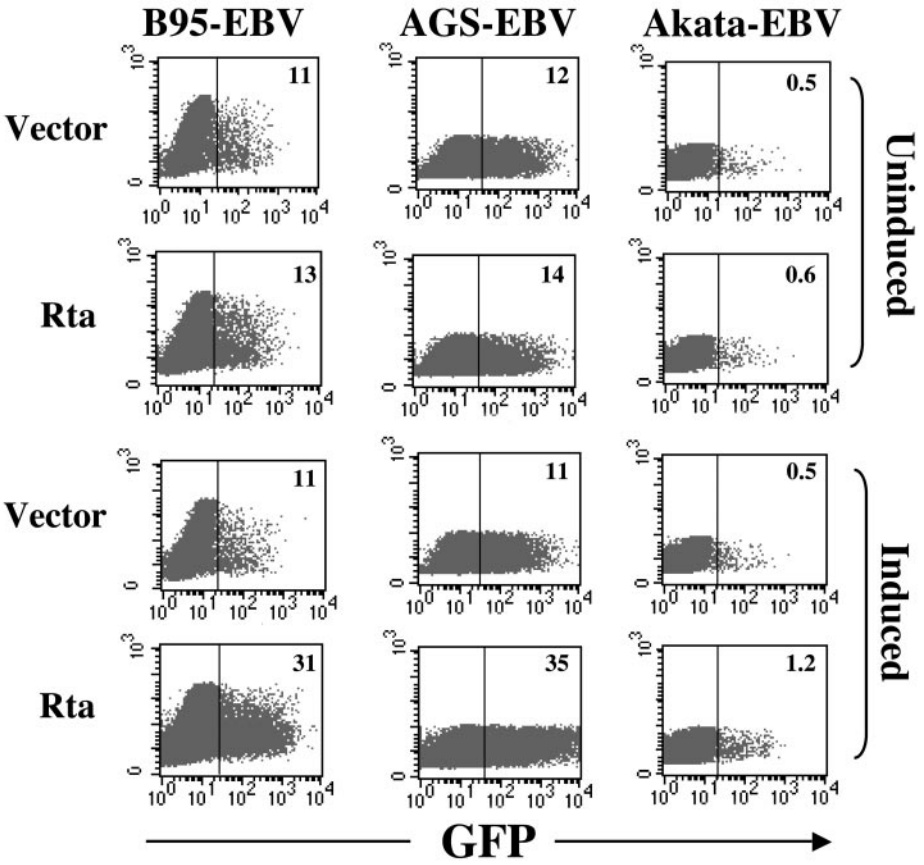

FIG. 4. Upregulation of RTA-induced CD21 expression facilitates EBV infection. EBVfaV-GFP from B95 B cells (B95-EBV-GFP), EBV-ΔTK-GFP from AGS epithelial cells (AGS-EBV-GFP), and EBV-ΔTK-GFP from Akata B cells (Akata-EBV-GFP) were obtained after 5 days of TPA or immunoglobulin stimulation and used to infect DOXY-induced or uninduced TRExBJAB-cDNA5 and TREXBJAB-RTA cells. At 48 h postinfection, EBV infectivity was determined with flow cytometry by measuring the GFP positivity of BJAB cells. The percentage of EBV-infected cells is shown in bold type in the top right-hand corner of each graph.

fluorescent protein (GFP) gene (36), AGS epithelial cells in which the thymidine kinase (TK) gene had been replaced with the GFP gene (1), and Akata B cells in which the thymidine kinase (TK) gene had been replaced with the GFP gene (1). EBVfaV-GFP from B95 B cells (B-EBV-GFP), EBV-ΔTK-GFP from AGS epithelial cells (E-EBV-GFP), and EBV-ΔTK-GFP from Akata B cells (Akata-EBV-GFP) were obtained after 5 days of TPA or Ig stimulation and used to infect DOXY-treated or untreated TRExBJAB-cDNA5 and TREx BJAB-RTA cells. At 48 h postinfection, EBV infectivity was assessed by measuring GFP fluorescence by flow cytometry. No significant difference in the infectivity of B95-EBV-GFP, AGS-EBV-GFP, and Akata-EBV-GFP viruses in TRExBJAB-cDNA5 and TREXBJAB-RTA cells was detected in cells that were not treated with DOXY (Fig. 4). In contrast, DOXY-treated TRExBJAB-RTA cells displayed considerably higher levels of EBV infection than DOXY-treated TRxBJAB-cDNA5 cells did; the levels of infection of B95-EBV-GFP and AGS-EBV-GFP viruses in DOXY-treated TRExBJAB-RTA cells were approximately threefold higher than that in DOXY-treated TRxBJAB-cDNA5 cells, and the level of infection of Akata-EBV-GFP virus in DOXY-treated TRExBJAB-RTA cells was twofold higher than that in DOXY-treated TRExBJAB-cDNA5 cells (Fig. 4). These results demonstrate that RTA-mediated upregulation of CD21 surface expression effectively facilitates EBV infection.

RTA activates CD23 gene expression through its RBP-Jκ binding site. Human CD23a is a B-cell differentiation marker involved in inflammatory responses. Analysis of the CD23a core promoter sequence reveals several binding sites for various cellular transcription factors, such as RBP-Jκ, Pax-5, and NF-κB (15). To identify the RTA-responsive sites in the CD23a promoter, we first used two CD23a promoter-luciferase reporter constructs CD23-ACP-Luc and CD23-AP-Luc. CD23-AP-Luc contains 1.2 kb of the CD23a promoter sequence, and CD23-ACP-Luc contains 283 bp of the CD23a core promoter sequence (41). TREx293-cDNA5, TREx293-RTA, TRExBJAB-cDNA5, and TRExBJAB-RTA cells were transfected with CD23-AP-Luc or CD23-ACP-Luc together with pGK-β-Gal and then treated with DOXY (1 μg/ml) or left alone. At 48 h posttransfection, cell lysates were used for reporter assays. RTA expression strongly activated promoter activities of both CD23-AP and CD23-ACP, indicating that the CD23a core promoter sequence is sufficient for RTA-induced activation (Fig. 5A). Precise inspection revealed five potential

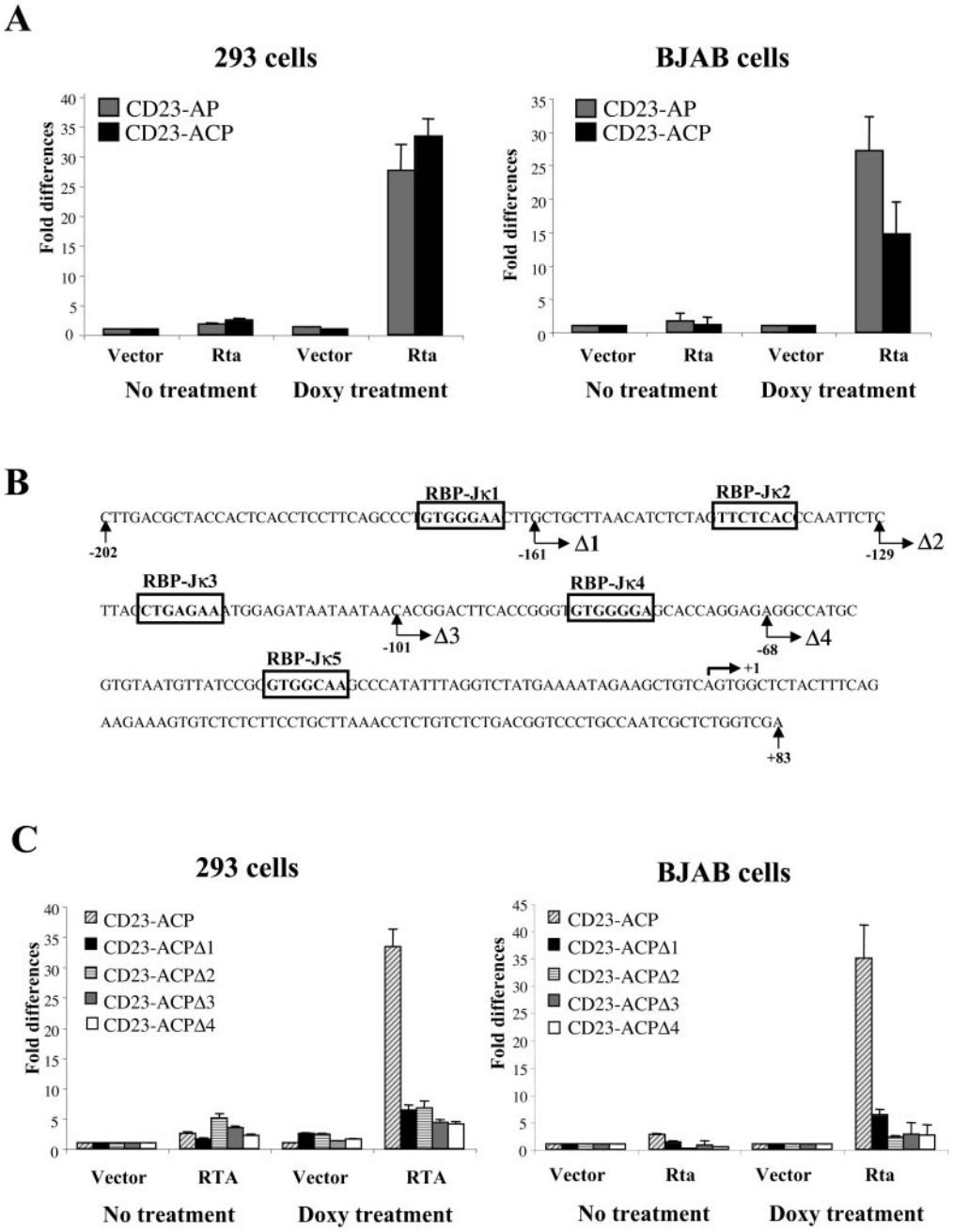

FIG. 5. Activation of CD23a gene expression induced by RTA. (A) CD23a core promoter sequence is sufficient for RTA-induced gene expression. TREx293-cDNA5, TREx293-RTA, TRExBJAB-cDNA5, and TRExBJAB-RTA cells were transfected with CD23-AP-Luc (CD23-AP) or CD23-ACP-Luc (CD23-ACP) together with pGK-β-Gal and then treated with DOXY (1 μg/ml) or left alone. At 48 h posttransfection, cell lysates were used for reporter assays. (B) Schematic diagram of the potential RBP-Jκ binding sites within the CD23a core. The five putative RBP-Jκ binding (GTGG/AGAA) sequences are shown in boxes. Numbers indicate the position relative to the transcription start site (+1). Arrows indicate the positions of each deletion mutation described in the text. (C) The first RBP-Jκ binding site of the CD23a core promoter sequence is primarily responsible for RTA-mediated activation. Wild-type or mutant CD23a promoter luciferase reporter (CD23-ACP or CD23-ACPΔ1 to CD23-ACPΔ4, respectively) together with the pGK-β-Gal construct was transfected into TREx293-cDNA5, TREx293-RTA, TRExBJAB-cDNA5, and TRExBJAB-RTA cells. The cells were then treated with DOXY (1 μg/ml) or left alone. At 48 h posttransfection, cell lysates were used for reporter assays. Luciferase activity is presented as the average ± standard deviation (error bar) of three independent experiments.

RBP-Jκ binding sites in the CD23a core promoter sequence (Fig. 5B).

To identify the RBP-Jκ elements in the CD23a core promoter region that are responsible for RTA activity, we generated luciferase reporter constructs containing serial deletion mutations at the CD23a core promoter sequence (Fig. 5B). These mutant reporters were Δ1, Δ2, Δ3, and Δ4, containing the sequences of the CD23a core promoter region from posi-

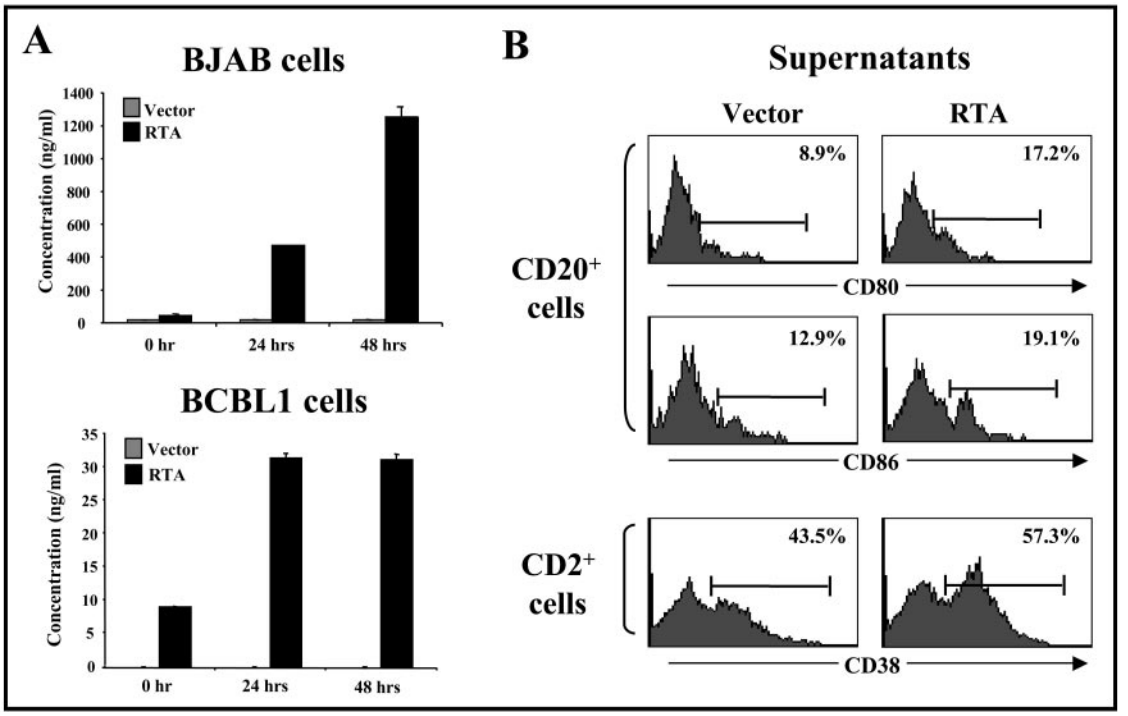

FIG. 6. sCD23 production by RTA and its effects on lymphocyte activation. (A) sCD23 production. TRExBJAB-cDNA5 and TRExBJAB-RTA cells and KSHV-infected TRExBCBL1-cDNA5 and TRExBLBL1-RTA cells were treated with DOXY (1 μg/ml) for 0, 24, and 48 h or left alone. Supernatants were collected and analyzed by ELISAs to measure the amount of sCD23. (B) sCD23 induces lymphocyte activation. Human PBMCs were treated with the supernatants from DOXY-stimulated TRExBJAB-cDNA5 or TRExBJAB-RTA cells. At 48 h, these cells were immunostained with an anti-CD21 antibody to identify B lymphocytes and with an anti-CD2 antibody to identify T lymphocytes. CD21-positive B lymphocytes were then further tested for the surface expression of CD80 and CD86, and CD2-postive T lymphocytes were tested for the surface expression of CD38. The black bars indicate the populations positive for CD80, CD86, or CD38 surface expression.

tions −161 to +83, −129 to +83, −101 to +83, and −68 to +83, respectively (positions relative to the transcription start site [+1]) (Fig. 5B). Wild-type or mutant CD23a promoter reporter constructs together with the pGK-β-Gal construct were transfected into TREx293-cDNA5, TREx293-RTA, TRExBJAB-cDNA5, and TRExBJAB-RTA cells, and these cells were then treated with DOXY (1 μg/ml) or left alone. At 48 h posttransfection, cell lysates were used for reporter assays. Deletion of the first RBP-Jκ binding site abolished RTA-mediated activation of CD23a promoter activity in both 293 and BJAB cells, indicating that the first RBP-Jκ binding site is principally responsible for the ability of RTA to induce CD23a gene expression (Fig. 5C).

sCD23 production by RTA. One of the hallmarks of B-cell chronic lymphocytic leukemia (B-CLL) cells is the overexpression of the transmembrane glycoprotein CD23, which undergoes proteolysis, giving rise to sCD23 molecules (15). In fact, the concentration of sCD23 in sera of B-CLL patients can be several hundredfold higher than in healthy individuals and is closely correlated with the clinical stage of the disease (15, 31, 33, 34). To determine whether RTA induced the production of sCD23, TRExBJAB-cDNA5 and TRExBJAB-RTA cells and KSHV-infected TRExBCBL1-cDNA5 and TRExBCBL1-RTA cells were treated with DOXY (1 μg/ml) for 24 and 48 h or left alone, and their supernatants were collected and analyzed by ELISAs to measure the amount of sCD23. Large amounts of sCD23 were detected in the supernatants of DOXY-treated TRExBJAB-RTA and TRExBCBL1-RTA cells, whereas almost no sCD23 was detected in the supernatants of TRExBJAB-cDNA5 and TRExBCBL1-cDNA5 cells with or without DOXY treatment (Fig. 6A). These results demonstrate that RTA expression in B cells and KSHV-infected PEL cells markedly induces sCD23 production.

Although CD23a was initially characterized as the low-affinity IgE receptor, it is involved in a variety of biological processes, such as IgE-dependent inflammatory processes and antigen presentation on B cells, and it is particularly important in homotypic or heterotypic interactions of T and B cells (41, 45). Furthermore, a recent study has demonstrated that sCD23 induced from macrophages by human immunodeficiency virus (HIV) Nef contributes to the induction of CD80 and CD86 surface expression on B cells and the HIV permissivity of resting T lymphocytes (39).

To investigate the potential biological effect of sCD23 on the activation of primary B and T lymphocytes, human peripheral blood mononuclear cells (PBMCs) were treated with the supernatants from DOXY-stimulated TRExBJAB-cDNA5 or TRExBJAB-RTA cells. At 48 h, the PBMCs were immunostained with an anti-CD21 antibody to identify B lymphocytes and an anti-CD2 antibody to identify T lymphocytes. CD21-positive B lymphocytes were then further tested for the expression of CD80 and CD86 costimulating molecules on the cell surface, and CD2-positive T lymphocytes were tested for the expression of the early T-lymphocyte activation marker CD38 on the cell surface. Flow cytometry showed that the levels of CD80 and CD86 expressed on the surfaces of primary B lym-

phocytes increased after treatment with the supernatants of TRExBJAB-RTA cells, whereas they were not affected by treatment with the supernatants of TRExBJAB-cDNA5 cells (Fig. 6B). Furthermore, expression of CD38 on the surfaces of primary T lymphocytes markedly increased after treatment with supernatants from TRExBJAB-RTA cells, whereas it was not altered after treatment with supernatants from TRExBJAB-cDNA5 cells (Fig. 6B). These results indicated that sCD23 produced by RTA expression induces the stimulation of primary B and T lymphocytes through the potential paracrine and autocrine pathways, which may facilitate homotypic or heterotypic interactions of T and B lymphocytes as seen in HIV-infected macrophages (39).

DISCUSSION

The KSHV RTA protein is responsible for the switch from latency to lytic replication, and this RTA activity requires its interaction with the RBP-Jκ transcription factor (18). Here, we demonstrate that RTA strongly induced CD21 and CD23a gene expression through the RBP-Jκ binding sites at the first intron region of CD21 and CD23a core promoter region, respectively. Furthermore, RTA-induced expression of CD21 surface glycoprotein effectively facilitated EBV infection, and RTA-induced expression of sCD23 glycoprotein activated primary human B and T lymphocytes. These results demonstrate that KSHV RTA regulates RBP-Jκ-mediated cellular gene expression, which ultimately provides a favorable milieu for viral reproduction in the infected host.

EBV EBNA2 contributes to B-cell immortalization, most likely by its ability to act as a transcriptional modulator of cellular and viral gene expression. It activates the transcription of B-cell activation markers CD21, CD23, and c-*myc* (42) and tyrosine kinase Fgr (43) and downregulates the expression of Igμ (37). EBNA2 does not bind to DNA directly but is recruited to EBNA2-responsive elements by interaction with RBP-Jκ transcription factor, indicating that EBNA2 is a functional homolog of the activated Notch protein (47). Indeed, cellular NIC has been shown to functionally substitute for EBNA2 in the context of EBV for primary B-cell transformation (7). However, the cellular targets of cellular NIC do not completely overlap with those of EBNA2: NIC and EBNA2 both activate CD21 gene expression and repress Igμ expression, whereas EBNA2, but not NIC, activates CD23a gene expression (37). We demonstrate that, like EBNA2, RTA activates CD21 and CD23a transcription. Interestingly, the first intronic sequence of CD21 has been shown to control appropriate B-cell-specific expression and also contain binding sites for RBP-Jκ and other transcription factors (25). In concordance with these findings, RTA-induced activation of CD21 promoter activity required the first intronic sequence. This was further confirmed by the requirement of the first intronic sequence of CD21 for NIC-mediated activation (unpublished results). Besides the previously characterized RBP-Jκ binding site of the CD23a core promoter region that EBV EBNA2 primarily targets (22), four additional sequences have also been shown to bind to RBP-Jκ (15). Our serial deletion mutational analysis showed that, as seen with EBNA2, the first RBP-Jκ binding sequence of the CD23 core promoter region was primarily responsible for RTA-induced activation. Despite this similarity between KSHV RTA and EBV EBNA2 for the activation of CD21 and CD23a gene expression, RTA does not affect Igμ and c-*myc* expression, which are strongly regulated by EBNA2. These results collectively indicate that KSHV RTA targets Notch signal transduction in a manner that is similar to but distinct from that of EBV EBNA2.

CD21 (also known as CR2, C3d, and EBV receptor) is a member of the regulators of complement activation gene family. CD21 is a B-cell receptor for CD23 and possibly for gamma interferon and also serves as the receptor for EBV gp350/220 (28). We demonstrate that the upregulation of CD21 surface expression induced by RTA facilitates EBV infection. Since most PEL cells are coinfected with KSHV and EBV, our results suggest the possibility of hierarchically ordered infection: KSHV infection, followed by EBV infection. This hypothesis is under active investigation.

CD23 (also known as low-affinity IgE receptor and FcεRII) is expressed as a type II extracellular protein on a variety of cells, such as B cells, monocytes, and macrophages, and is cleaved from the cell surface to generate several distinct fragments. This cleavage is mediated by a metalloprotease. This sCD23 then acts as a B-cell growth factor and is associated with EBV infection (15). In fact, since the level of sCD23 in serum is higher in patients with autoimmune diseases and B-CLL, it has been used as an indicator of the progression of disease (15, 31, 34). This suggests the intriguing possibility that KSHV-infected PEL patients may also have high levels of sCD23 in serum. Unfortunately, the limited availability of sera from PEL patients did not allow us to determine the levels of sCD23 in sera from PEL patients. Nevertheless, it will be interesting to pursue whether KSHV infection is associated with a high level of sCD23 in serum, which may provide a marker for KSHV infection and progression.

A recent study has demonstrated that sCD23 and soluble ICAM1, which are induced from macrophages by HIV Nef, contribute to the induction of the expression of CD80 and CD86 on the surfaces of B cells and the HIV permissivity of resting T lymphocytes (39). We also showed that the expression of CD80 and CD86 costimulating molecules on the surfaces of primary B lymphocytes and the CD38 activation marker on primary T lymphocytes increased after treatment with the supernatants of TRExBJAB-RTA cells, whereas it was not affected after treatment with the supernatants of TRExBJAB-cDNA5 cells. These results suggest that sCD23 produced by RTA expression induces the stimulation of primary B and T cells through the potential paracrine and autocrine pathways, which may ultimately facilitate homotypic or heterotypic interactions of T and B cells. This also suggests that KSHV RTA potentially influences the activation state of infected B cells, thereby enhancing the ability of neighboring T cells to support the replication of HIV type 1. This activity may require the upregulation of CD80 and CD86 B-cell costimulating receptors involved in the alternative pathway of T-lymphocyte stimulation. Thus, although the full significance of RTA-mediated effects on the other coexisting viruses in KS and PEL patients needs to be studied further, our study may provide insight into the comprehensive mechanism by which KSHV RTA not only activates lytic reactivation by targeting KSHV gene expression but also creates a favorable milieu for viral infection and replication by activating cellular gene expression.

ACKNOWLEDGMENTS

We thank R. Longnecker, P. Ling, D. Hayward, H. P. Tony, and J. H. Weis for providing cells and reagents and J. Macke for reading and editing the manuscript.

This work was partly supported by U.S. Public Health Service grants CA115284, CA106156, CA91819, CA082057, and RR00168. J. U. Jung is a Leukemia & Lymphoma Society Scholar.

REFERENCES

1. **Borza, C. M., and L. M. Hutt-Fletcher.** 2002. Alternate replication in B cells and epithelial cells switches tropism of Epstein-Barr virus. Nat. Med. **8:**594–599.
2. **Boshoff, C., T. F. Schulz, M. M. Kennedy, A. K. Graham, C. Fisher, A. Thomas, J. O. McGee, R. A. Weiss, and J. J. O'Leary.** 1995. Kaposi's sarcoma-associated herpesvirus infects endothelial and spindle cells. Nat. Med. **1:**1274–1278.
3. **Cesarman, E., Y. Chang, P. S. Moore, J. W. Said, and D. M. Knowles.** 1995. Kaposi's sarcoma-associated herpesvirus-like DNA sequences in AIDS-related body-cavity-based lymphomas. N. Engl. J. Med. **332:**1186–1191.
4. **Chang, Y., E. Cesarman, M. S. Pessin, F. Lee, J. Culpepper, D. M. Knowles, and P. S. Moore.** 1994. Identification of herpesvirus-like DNA sequences in AIDS-associated Kaposi's sarcoma. Science **266:**1865–1869.
5. **Coscoy, L., and D. Ganem.** 2001. A viral protein that selectively downregulates ICAM-1 and B7-2 and modulates T cell costimulation. J. Clin. Investig. **107:**1599–1606.
6. **Fingeroth, J. D., J. J. Weis, T. F. Tedder, J. L. Strominger, P. A. Biro, and D. T. Fearon.** 1984. Epstein-Barr virus receptor of human B lymphocytes is the C3d receptor CR2. Proc. Natl. Acad. Sci. USA **81:**4510–4514.
7. **Gordadze, A. V., R. Peng, J. Tan, G. Liu, R. Sutton, B. Kempkes, G. W. Bornkamm, and P. D. Ling.** 2001. Notch1IC partially replaces EBNA2 function in B cells immortalized by Epstein-Barr virus. J. Virol. **75:**5899–5912.
8. **Gradoville, L., J. Gerlach, E. Grogan, D. Shedd, S. Nikiforow, C. Metroka, and G. Miller.** 2000. Kaposi's sarcoma-associated herpesvirus open reading frame 50/Rta protein activates the entire viral lytic cycle in the HH-B2 primary effusion lymphoma cell line. J. Virol. **74:**6207–6212.
9. **Gwack, Y., H. J. Baek, H. Nakamura, S. H. Lee, M. Meisterernst, R. G. Roeder, and J. U. Jung.** 2003. Principal role of TRAP/mediator and SWI/SNF complexes in Kaposi's sarcoma-associated herpesvirus RTA-mediated lytic reactivation. Mol. Cell. Biol. **23:**2055–2067.
10. **Gwack, Y., H. Byun, S. Hwang, C. Lim, and J. Choe.** 2001. CREB-binding protein and histone deacetylase regulate the transcriptional activity of Kaposi's sarcoma-associated herpesvirus open reading frame 50. J. Virol. **75:**1909–1917.
11. **Gwack, Y., S. Hwang, C. Lim, Y. S. Won, C. H. Lee, and J. Choe.** 2002. Kaposi's sarcoma-associated herpesvirus open reading frame 50 stimulates the transcriptional activity of STAT3. J. Biol. Chem. **277:**6438–6442.
12. **Hamaguchi, Y., Y. Yamamoto, H. Iwanari, S. Maruyama, T. Furukawa, N. Matsunami, and T. Honjo.** 1992. Biochemical and immunological characterization of the DNA binding protein (RBP-J kappa) to mouse J kappa recombination signal sequence. J. Biochem. (Tokyo) **112:**314–320.
13. **Hsieh, J. J., and S. D. Hayward.** 1995. Masking of the CBF1/RBPJ kappa transcriptional repression domain by Epstein-Barr virus EBNA2. Science **268:**560–563.
14. **Hu, H., B. K. Martin, J. J. Weis, and J. H. Weis.** 1997. Expression of the murine CD21 gene is regulated by promoter and intronic sequences. J. Immunol. **158:**4758–4768.
15. **Hubmann, R., J. D. Schwarzmeier, M. Shehata, M. Hilgarth, M. Duechler, M. Dettke, and R. Berger.** 2002. Notch2 is involved in the overexpression of CD23 in B-cell chronic lymphocytic leukemia. Blood **99:**3742–3747.
16. **Ishido, S., C. Wang, B. S. Lee, G. B. Cohen, and J. U. Jung.** 2000. Downregulation of major histocompatibility complex class I molecules by Kaposi's sarcoma-associated herpesvirus K3 and K5 proteins. J. Virol. **74:**5300–5309.
17. **Kawaichi, M., C. Oka, S. Shibayama, A. E. Koromilas, N. Matsunami, Y. Hamaguchi, and T. Honjo.** 1992. Genomic organization of mouse J kappa recombination signal binding protein (RBP-J kappa) gene. J. Biol. Chem. **267:**4016–4022.
18. **Liang, Y., J. Chang, S. J. Lynch, D. M. Lukac, and D. Ganem.** 2002. The lytic switch protein of KSHV activates gene expression via functional interaction with RBP-Jκ (CSL), the target of the Notch signaling pathway. Genes Dev. **16:**1977–1989.
19. **Liang, Y., and D. Ganem.** 2004. RBP-J (CSL) is essential for activation of the K14/vGPCR promoter of Kaposi's sarcoma-associated herpesvirus by the lytic switch protein RTA. J. Virol. **78:**6818–6826.
20. **Liao, W., Y. Tang, Y. L. Kuo, B. Y. Liu, C. J. Xu, and C. Z. Giam.** 2003. Kaposi's sarcoma-associated herpesvirus/human herpesvirus 8 transcriptional activator Rta is an oligomeric DNA-binding protein that interacts with tandem arrays of phased A/T-trinucleotide motifs. J. Virol. **77:**9399–9411.
21. **Ling, P. D., and S. D. Hayward.** 1995. Contribution of conserved amino acids in mediating the interaction between EBNA2 and CBF1/RBPJk. J. Virol. **69:**1944–1950.
22. **Ling, P. D., J. J. Hsieh, I. K. Ruf, D. R. Rawlins, and S. D. Hayward.** 1994. EBNA-2 upregulation of Epstein-Barr virus latency promoters and the cellular CD23 promoter utilizes a common targeting intermediate, CBF1. J. Virol. **68:**5375–5383.
23. **Lukac, D. M., R. Renne, J. R. Kirshner, and D. Ganem.** 1998. Reactivation of Kaposi's sarcoma-associated herpesvirus infection from latency by expression of the ORF 50 transactivator, a homolog of the EBV R protein. Virology **252:**304–312.
24. **Makar, K. W., C. T. Pham, M. H. Dehoff, S. M. O'Connor, S. M. Jacobi, and V. M. Holers.** 1998. An intronic silencer regulates B lymphocyte cell- and stage-specific expression of the human complement receptor type 2 (CR2, CD21) gene. J. Immunol. **160:**1268–1278.
25. **Makar, K. W., D. Ulgiati, J. Hagman, and V. M. Holers.** 2001. A site in the complement receptor 2 (CR2/CD21) silencer is necessary for lineage specific transcriptional regulation. Int. Immunol. **13:**657–664.
26. **Nador, R. G., E. Cesarman, A. Chadburn, D. B. Dawson, M. Q. Ansari, J. Sald, and D. M. Knowles.** 1996. Primary effusion lymphoma: a distinct clinicopathologic entity associated with the Kaposi's sarcoma-associated herpes virus. Blood **88:**645–656.
27. **Nakamura, H., M. Lu, Y. Gwack, J. Souvlis, S. L. Zeichner, and J. U. Jung.** 2003. Global changes in Kaposi's sarcoma-associated virus gene expression patterns following expression of a tetracycline-inducible Rta transactivator. J. Virol. **77:**4205–4220.
28. **Nemerow, G. R., C. Mold, V. K. Schwend, V. Tollefson, and N. R. Cooper.** 1987. Identification of gp350 as the viral glycoprotein mediating attachment of Epstein-Barr virus (EBV) to the EBV/C3d receptor of B cells: sequence homology of gp350 and C3 complement fragment C3d. J. Virol. **61:**1416–1420.
29. **Nemerow, G. R., R. Wolfert, M. E. McNaughton, and N. R. Cooper.** 1985. Identification and characterization of the Epstein-Barr virus receptor on human B lymphocytes and its relationship to the C3d complement receptor (CR2). J. Virol. **55:**347–351.
30. **Radtke, F., and K. Raj.** 2003. The role of Notch in tumorigenesis: oncogene or tumour suppressor? Nat. Rev. Cancer **3:**756–767.
31. **Reinisch, W., M. Willheim, M. Hilgarth, C. Gasche, R. Mader, S. Szepfalusi, G. Steger, R. Berger, K. Lechner, G. Boltz-Nitulescu, et al.** 1994. Soluble CD23 reliably reflects disease activity in B-cell chronic lymphocytic leukemia. J. Clin. Oncol. **12:**2146–2152.
32. **Sakakibara, S., K. Ueda, J. Chen, T. Okuno, and K. Yamanishi.** 2001. Octamer-binding sequence is a key element for the autoregulation of Kaposi's sarcoma-associated herpesvirus ORF50/Lyta gene expression. J. Virol. **75:**6894–6900.
33. **Schroeder, J. R., A. J. Saah, R. F. Ambinder, O. Martinez-Maza, E. Crabb Breen, D. Variakojis, J. B. Margolick, L. P. Jacobson, D. T. Rowe, and D. R. Hoover.** 1999. Serum sCD23 level in patients with AIDS-related non-Hodgkin's lymphoma is associated with absence of Epstein-Barr virus in tumor tissue. Clin. Immunol. **93:**239–244.
34. **Schwarzmeier, J. D., M. Shehata, M. Hilgarth, I. Marschitz, N. Louda, R. Hubmann, and R. Greil.** 2002. The role of soluble CD23 in distinguishing stable and progressive forms of B-chronic lymphocytic leukemia. Leuk. Lymphoma **43:**549–554.
35. **Song, M. J., X. Li, H. J. Brown, and R. Sun.** 2002. Characterization of interactions between RTA and the promoter of polyadenylated nuclear RNA in Kaposi's sarcoma-associated herpesvirus/human herpesvirus 8. J. Virol. **76:**5000–5013.
36. **Speck, P., and R. Longnecker.** 1999. Epstein-Barr virus (EBV) infection visualized by EGFP expression demonstrates dependence on known mediators of EBV entry. Arch. Virol. **144:**1123–1137.
37. **Strobl, L. J., H. Hofelmayr, G. Marschall, M. Brielmeier, G. W. Bornkamm, and U. Zimber-Strobl.** 2000. Activated Notch1 modulates gene expression in B cells similarly to Epstein-Barr viral nuclear antigen 2. J. Virol. **74:**1727–1735.
38. **Sun, R., S. F. Lin, L. Gradoville, Y. Yuan, F. Zhu, and G. Miller.** 1998. A viral gene that activates lytic cycle expression of Kaposi's sarcoma-associated herpesvirus. Proc. Natl. Acad. Sci. USA **95:**10866–10871.
39. **Swingler, S., B. Brichacek, J. M. Jacque, C. Ulich, J. Zhou, and M. Stevenson.** 2003. HIV-1 Nef intersects the macrophage CD40L signalling pathway to promote resting-cell infection. Nature **424:**213–219.
40. **Ulgiati, D., and V. M. Holers.** 2001. CR2/CD21 proximal promoter activity is critically dependent on a cell type-specific repressor. J. Immunol. **167:**6912–6919.
41. **Visan, I., M. Goller, I. Berberich, C. Kneitz, and H. P. Tony.** 2003. Pax-5 is a key regulator of the B cell-restricted expression of the CD23a isoform. Eur. J. Immunol. **33:**1163–1173.
42. **Wang, F., C. D. Gregory, M. Rowe, A. B. Rickinson, D. Wang, M. Birkenbach, H. Kikutani, T. Kishimoto, and E. Kieff.** 1987. Epstein-Barr virus nuclear antigen 2 specifically induces expression of the B-cell activation antigen CD23. Proc. Natl. Acad. Sci. USA **84:**3452–3456.
43. **Wang, F., H. Kikutani, S. F. Tsang, T. Kishimoto, and E. Kieff.** 1991. Epstein-Barr virus nuclear protein 2 transactivates a *cis*-acting CD23 DNA element. J. Virol. **65:**4101–4106.
44. **Wang, S., S. Liu, M. H. Wu, Y. Geng, and C. Wood.** 2001. Identification of a

cellular protein that interacts and synergizes with the RTA (ORF50) protein of Kaposi's sarcoma-associated herpesvirus in transcriptional activation. J. Virol. **75:**11961–11973.

45. **Yokota, A., H. Kikutani, T. Tanaka, R. Sato, E. L. Barsumian, M. Suemura, and T. Kishimoto.** 1988. Two species of human Fc epsilon receptor II (Fc epsilon RII/CD23): tissue-specific and IL-4-specific regulation of gene expression. Cell **55:**611–618.
46. **Zabel, M. D., W. Wheeler, J. J. Weis, and J. H. Weis.** 2002. Yin Yang 1, Oct1, and NFAT-4 form repeating, cyclosporin-sensitive regulatory modules within the murine CD21 intronic control region. J. Immunol. **168:** 3341–3350.
47. **Zimber-Strobl, U., and L. J. Strobl.** 2001. EBNA2 and Notch signalling in Epstein-Barr virus mediated immortalization of B lymphocytes. Semin. Cancer Biol. **11:**423–434.